ELSEVIER

Journal of Alloys and Compounds 444–445 (2007) 598–602

Journal of ALLOYS AND COMPOUNDS

www.elsevier.com/locate/jallcom

Diffuse reflectance spectroscopy of neptunium ions in polycrystalline ceramics designed for immobilization of HLW

Yingjie Zhang*, Eric R. Vance, Bruce D. Begg, Huijun Li

Australian Nuclear Science and Technology Organisation, PMB 1, Menai, NSW 2234, Australia

Received 30 June 2006; received in revised form 11 January 2007; accepted 12 January 2007

Abstract

Diffuse reflectance spectra at room temperature have been collected on polycrystalline perovskite ($CaTiO_3$), zirconolite ($CaZrTi_2O_7$) and thorutite ($ThTi_2O_6$) samples doped with Np. The Np species give rise to a number of broad, unresolved intraconfigurational *f–f* electronic transition bands in the near-infrared and visible spectral regions.

Both Np^{3+} and Np^{4+} can substitute in the Ca site of perovskite by the appropriate choice of charge compensation and sintering atmosphere. No detectable spectral differences were observed when Np^{4+} was targeted towards either the Ca or Zr sites in zirconolite. Np^{4+} but not Np^{5+} can be incorporated in the Th site of thorutite by sintering in air. Even in the most dilute [≤ 0.03 formula units (f.u.)] Np^{4+} samples of the different titanates studied, there was only very approximate agreement with the Kubelka–Munk law.

Keywords: Diffuse reflectance spectroscopy; Neptunium; Titanate ceramics

1. Introduction

The immobilization of actinide-rich radioactive wastes in durable matrices and long-term safe geological isolation of such waste forms is a globally important environmental issue. Titanate-based ceramics, namely synroc, have been shown to be eminently appropriate for immobilization of Pu-rich materials [1]. In the last decade, synroc formulations targeting various high-level waste (HLW) streams have been developed [2–5] and their long-term chemical durabilities have been extensively studied [6–8]. In the typical synroc-C formulation, designed for high-level Purex reprocessing waste, actinides are incorporated mainly in durable perovskite ($CaTiO_3$) and zirconolite ($CaZrTi_2O_7$) crystal lattices. Brannerite (UTi_2O_6), another durable titanate mineral phase, was also present as a minor actinide-bearing phase in the pyrochlore-rich formulations designed for immobilization of surplus Pu [1].

Generally the light actinides can adopt various oxidation states subject to the availability of appropriate charge compensators, crystal-field stabilisation energy and the actual processing redox conditions. Therefore, the direct determination of actinide oxidation states is an important routine practice for wasteform development.

X-ray absorption spectroscopy (XAS), scanning electron microscope (SEM) and X-ray diffraction (XRD) have previously been used to study neptunium valences in perovskite and zirconolite [9,10]. Both Np^{3+} and Np^{4+} have been identified in perovskite [9] and it is necessary to use reducing conditions with appropriate charge compensations to achieve Np^{3+} [10].

Brannerite, UTi_2O_6, can only be synthesised in pure form under low oxygen partial pressure [11]. However, U^{5+} has been stabilised by using Ca^{2+} or Y^{3+} as charge compensators on the Th site of thorutite ($ThTi_2O_6$) sintered in air or argon [12,13], with U^{4+} also being present. In view of this, it is of interest to examine whether higher valence states than Np^{4+} can also be stabilised in the brannerite structure.

Transmission optical spectroscopy at low temperatures can be used to study the electronic structure of actinide ions in solid materials if suitable transparent single crystals are available. However, in the absence of such single crystals, diffuse reflectance spectroscopy (DRS) has been found to be one of the useful tools to derive uranium and plutonium ion valences in some of the titanate ceramic phases [12–14]. In the present work, DR spectra of perovskite, zirconolite and thorutite

---

* Corresponding author. Tel.: +61 2 9717 9156; fax: +61 2 9543 7179.
E-mail address: yzx@ansto.gov.au (Y. Zhang).

0925-8388/$ – see front matter. Crown Copyright © 2007 Published by Elsevier B.V. All rights reserved.
doi:10.1016/j.jallcom.2007.01.055

samples containing various amounts of Np were collected over the near-infrared (NIR) and visible range (4000–25000 cm^{-1}) to assist the definition of Np valences in these polycrystalline materials. Electronic absorption is expected in this spectral region for $Np^{3+}(f^4)$, $Np^{4+}(f^3)$ and $Np^{5+}(f^2)$ ions, arising from intraconfigurational *f–f* transitions [15–18]. Bandshifts and possible band splittings are also expected on doping of Np ions into crystalline oxide lattices and the actual absorption band intensities will largely depend on the Np local symmetry.

In the literature, little theoretical modelling of Np^{3+} and Np^{4+} spectra in the condensed phase with well-defined symmetry character has been attempted [15–18]. The complexity of Np^{3+} and Np^{4+} spectra arising from transitions within partly filled 5*f* shell is mainly due to the fact that there is a large number of free-ion states which lie close to one another and which are further split by crystal fields being of the same order of magnitude as the interelectronic repulsion and the spin-orbit coupling [18]. In addition, different splitting patterns and transition intensities arising from different site-symmetries and selection rules are probably only detectable in low temperature spectra. Therefore, in this work we only focussed on spectral features and intersample comparisons rather than spectral assignments.

2. Experimental

2.1. Materials

The polycrystalline perovskite and zirconolite samples were made by the standard alkoxide/nitrate route [2] and sintered at 1400 °C for 20 h under different atmospheres. Samples were characterised by XRD and SEM and found to be essentially single-phase.

The Np-doped thorutite ($ThTi_2O_6$) samples were prepared in the same way as for perovskite and zirconolite but sintered at 1450 °C for 20 h in air. In one case for thorutite, yttrium was added as a charge compensator to favour the formation of Np^{5+} (U^{5+} was successfully stabilised in thorutite under the same conditions [12]).

2.2. Scanning electron microscope and diffuse reflectance spectroscopy

Scanning electron microscopy (SEM) was carried out with a JEOL JSM-6300 instrument operated at 15 kV, and fitted with a NORAN Voyager IV X-ray microanalysis system (EDX). Calibrations for microanalysis were carried out using a comprehensive set of standards for quantitative analysis [19].

Diffuse reflectance spectra of the sintered ceramics were measured at ambient temperature using a Cary 500 spectrophotometer equipped with a Labsphere Biconical Accessory, which employs a beam spot size of approximately 1 mm in diameter. Absorption spectra were referenced to a Labsphere certified standard (Spectralon) and then transformed into Kubelka–Munk units, $F(R) = (1-R)^2/2R$ [20].

3. Results and discussion

3.1. Np ions in perovskite

Fig. 1 shows DR spectra, in the NIR region, of $Ca_{1-x}Np_x Ti_{1-2x}Al_{2x}O_3$ perovskite samples sintered in air with Np targeted to have Np^{4+} on the Ca site. The spectra are very similar to the solution spectrum of Np^{4+} [17] but have better resolved bands. The similarity of absorption spectra of Np^{4+} in aqueous solution and polycrystalline perovskite suggests that in perovskite the crystal field effects are relatively weak. Note the Ca site in perovskite has orthorhombic point symmetry with a coordination number of 12. The Kubelka–Munk law is only roughly obeyed at low Np^{4+} doping levels (Fig. 1). Although the band intensities increase with Np content, they increase less than linearly, especially for the bands in the 10000–12000 cm^{-1} spectral region.

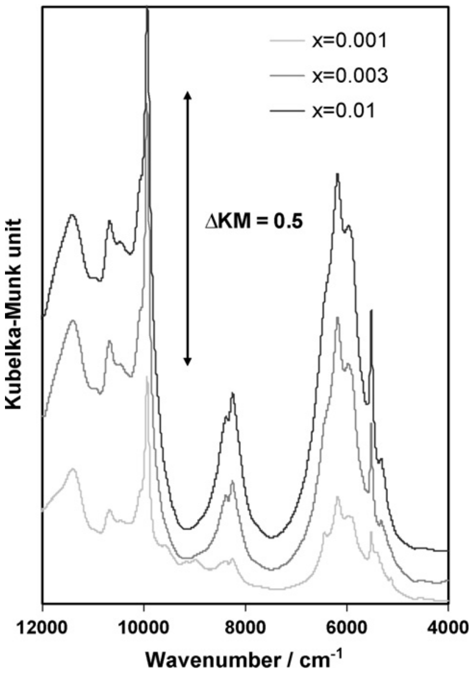

Fig. 1. DR spectra (4000–12000 cm^{-1}) of Np^{4+} in perovskite ($Ca_{1-x}Np_xTi_{1-2x}Al_{2x}O_3$) sintered in air showing spectra scaling up with increasing Np concentration (*x*) (spectra offset vertically to enhance visibility).

The DR spectra of Np on the Ca site of perovskite with or without Al charge compensators sintered in air are shown in Fig. 2. The two spectra resemble each other very well with hardly any band shifts and only slightly band-shape differences probably caused by the addition of charge compensators. The similarity indicates that sintering samples in air always gave rise to the formation of Np^{4+} in $CaTiO_3$ irrespective of whether Al charge compensators were added. The charge compensation in the Al-free samples probably takes place by cation vacancy formation, by analogy with $Ca_{1-x}La_xTiO_3$ perovskites [21]. However, although the weak bands at around 4400 and 7200 cm^{-1} suggest that there might be some Np^{3+} present in both samples, a previous study showed that air or neutral atmospheres are inadequate to produce Np^{3+} in perovskite [10].

Reduction of perovskite samples by heating in 3.5% H_2/N_2 atmosphere to produce Np^{3+} generally led to increased general absorption (with the samples turning black in color) and broadly featureless spectra, obliterating any weak Np^{3+} absorptions in samples dilute in Np. However, for samples containing 0.1 f.u. of Np (Fig. 3), characteristic absorption peaks for Np^{3+} at around 4400 cm^{-1} could be detected for both samples, with or without Al on Ti-site as charge compensators.

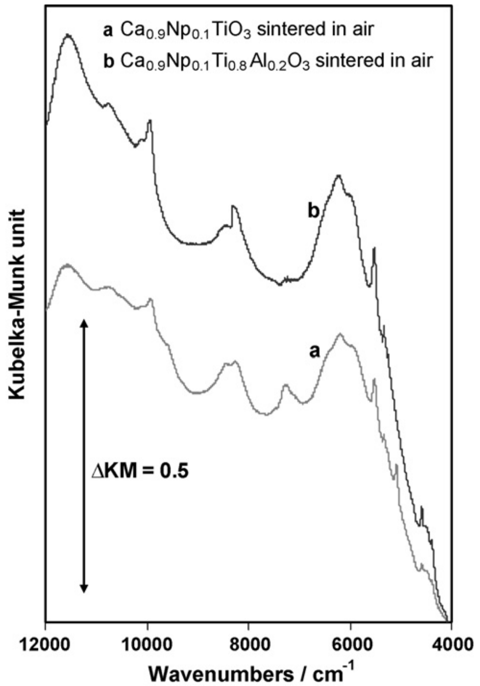

Fig. 2. DR spectra (4000–12000 cm^{-1}) of Np in perovskite sintered in air with or without Al on Ti site as charge compensators (spectra offset vertically to enhance visibility).

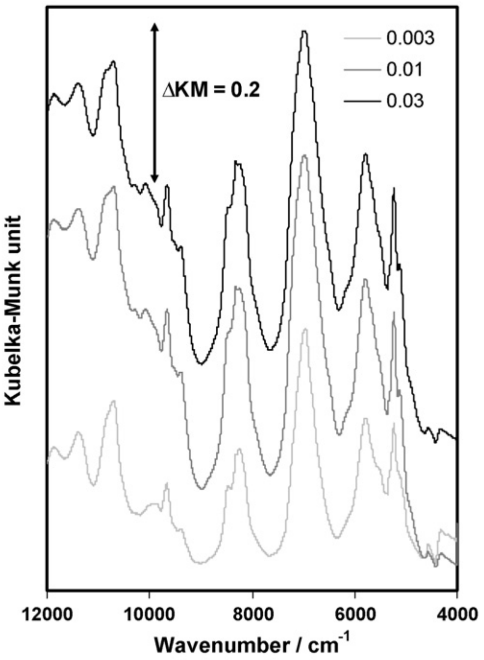

Fig. 4. DR spectra (4000–12000 cm^{-1}) of Np^{4+} in zirconolite ($CaNp_xZr_{1-x}Ti_2O_7$) sintered in air showing spectra scaling up with increasing of Np concentrations (x) (spectra offset vertically to enhance visibility).

3.2. Np ions in zirconolite

Np^{4+} incorporation in zirconolite at doping levels of ≥0.1 f.u. has been shown to proceed by (a) direct substitution in the Zr site or (b) substitution in the Ca site with compensation via 2 Al (or Ga/In) ions substituted for Ti for each Np^{4+} ion [10]. However, at doping levels of ∼0.01 f.u. or less, reliance on the overall sample composition is difficult and more direct techniques such as electron paramagnetic resonance would be necessary (Np^{4+} is a Kramers ion). In the present work, the Np^{4+} ions were only targeted to Ca or Zr sites via the overall composition.

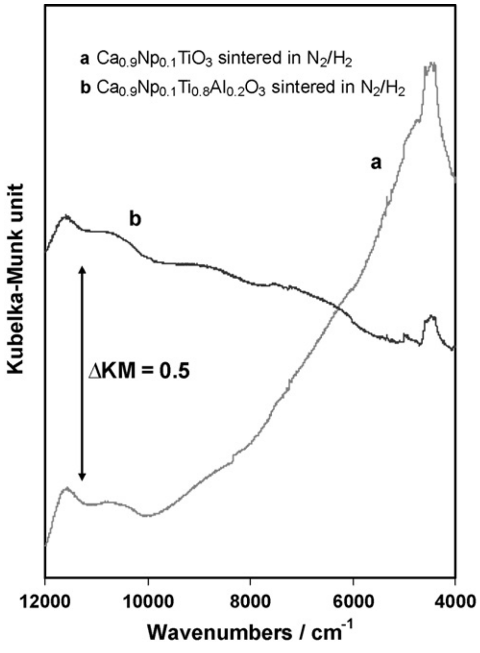

Fig. 3. DR spectra (4000–12000 cm^{-1}) of Np in perovskite sintered in 3.5% H_2/N_2 with or without Al on Ti site as charge compensators (spectra offset vertically to enhance visibility).

Fig. 4 shows DR spectra, in the NIR region, of zirconolite samples sintered in air with Np^{4+} [10] targeted on the Ca site. The spectra are similar to those of Np-doped perovskite except for an additional sharp and strong transition band at around 7000 cm^{-1}. A previous study [22] of the absorption spectrum of Np in ThO_2 implied that a band at around 7100 cm^{-1} was due to Np^{3+} but ongoing work in this laboratory suggests that this assignment is unlikely. In any case, Np is only present in tetravalent form (see above) in Np-doped zirconolite sintered in air. Therefore the transition bands at around 7000 cm^{-1} are most likely due to the lower Np site symmetry in zirconolite, as compared to ThO_2. The Ca and Zr sites in zirconolite have 8- and 7-fold coordinations, respectively, with no symmetry elements other than the identity operator. The absorption bands generally increased in intensity only marginally with the increase of Np concentration in zirconolite.

Np^{4+} targeting either the Ca or Zr sites of zirconolite gave very little difference on the absorption spectra (not shown). Evidently the crystal field splittings in the two kinds of sites cannot be distinguished due to the band broadening at ambient temperature. This is consistent with our early work, in which we had found that DR spectra of U^{4+} and Pu^{4+} in zirconolite collected at ambient temperature were essentially indistinguishable when they were targeted towards either the Ca or Zr sites in zirconolite [23,14].

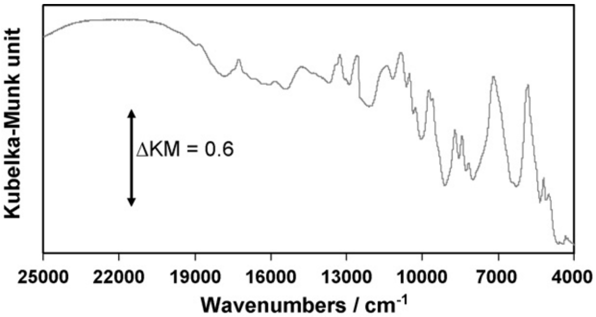

Fig. 5. DR spectrum (4000–25000 cm^{-1}) of Np^{4+} in thorutite ($Np_{0.2}Th_{0.8}Ti_2O_6$) sintered in air.

3.3. *Np ions in Th-brannerite*

A DR spectrum of Np^{4+} in thorutite over the NIR/visible region is shown in Fig. 5. It is fairly similar to the DR spectra of Np^{4+} in zirconolite (Fig. 4), with minor bandshifts and splittings. Brannerite belongs to the monoclinic crystal system and actinides occupy distorted octahedral coordination with a centre of inversion (actinide site symmetry C_{2h}). Attempts to prepare Np^{5+} in thorutite by adding Y^{3+} on Th site as charge compensators was unsuccessful insofar as the spectrum was the same as that of Np^{4+}, suggesting that Np^{4+} is strongly favoured over Np^{5+} in air-fired conditions even in the presence of appropriate charge compensators for the formation of Np^{5+}.

The DR spectra of Np^{4+} in perovskite, zirconolite and brannerite structures are all shown together for comparison in Fig. 6. In general, they are similar at higher wave numbers (>8000 cm^{-1}). However, the differences (bandshifts, splittings and additional bands) at lower wave numbers (<8000 cm^{-1}) clearly reflect different Np^{4+} local site symmetries in the three crystal lattices.

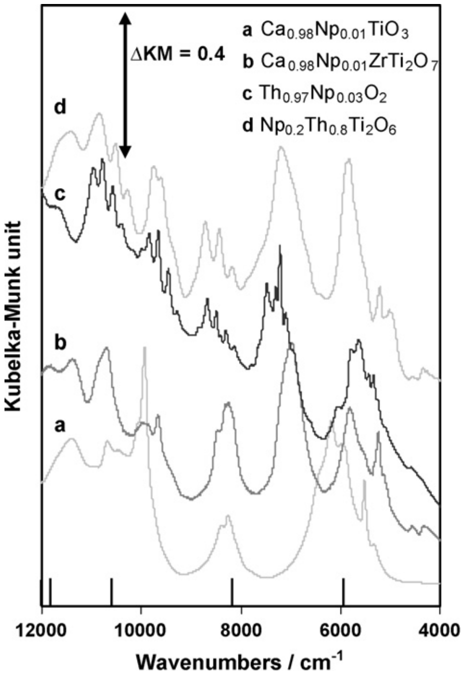

Fig. 6. DR spectra (4000–12000 cm^{-1}) of Np^{4+} (free-ion energy levels shown at the bottom) in perovskite, zirconolite, thoria and thorutite sintered in air (spectra offset vertically to enhance visibility).

4. Conclusions and final remarks

DR spectroscopy has been used to study Np ion valences in perovskite, zirconolite and brannerite, complementary to earlier XANES work [10]. Sintering these samples in air or argon always gives rise to the formation of Np^{4+}. Np^{3+} can be formed at reducing conditions (firing in H_2-bearing atmospheres) in perovskite whilst zirconolite cannot form as a single-phase under these conditions. There is no evidence of Np^{5+} in thorutite sintered in air, even with Y^{3+} ions added as charge compensators. This is distinct from U, where U^{5+} was observed when appropriate charge compensation was present in air-fired samples [12,13]. The intensities of the Np^{4+} absorption peaks increased with increasing Np content, but did not strictly follow the Kubelka–Munk law even over the low Np concentration range (0.003–0.03 f.u.). Like previous observations for U^{4+} and Pu^{4+} in zirconolite [23,14], there appeared to be little difference in the electronic spectra between Np^{4+} in the Ca versus the Zr site of zirconolite as the crystal field splittings in the two kinds of sites cannot be distinguished at ambient temperature due to the band broadening and overlapping. Overall, DR spectroscopy is capable of identifying Np valences in polycrystalline titanate ceramics. Np^{3+} spectra in monazite are under study.

Acknowledgements

We are indebted to A. Brownscombe and T. McLeod for fabricating the samples.

References

[1] B.B. Ebbinghaus, R.A. Vankonynenburg, F.J. Ryerson, E.R. Vance, M.W.A. Stewart, A. Jostsons, J.S. Allender, T. Rankin, J. Congdon, Waste Management'98 (CD-ROM; sess65/65-04), WM Symposia Inc., Tucson, AZ, 1998.

[2] A.E. Ringwood, S.E. Kesson, K.D. Reeve, D.M. Levins, E.J. Ramm, in: W. Lutze, R.C. Ewing (Eds.), Radioactive Waste Forms for the Future, Elsevier, Netherlands, 1988, pp. 233–334.

[3] E.R. Vance, Mater. Res. Soc. MRS Bull. XIX (1994) 28–32.

[4] E.R. Vance, A. Jostsons, S. Moricca, M.W.A. Stewart, R.A. Day, B.D. Begg, M.J. Hambley, K.P. Hart, B.B. Ebbinghaus, in: J.C. Marra, G.T. Chandler (Eds.), Environmental Issues and Waste Management Technologies in the Ceramic and Nuclear Industries IV, American Ceramic Society, Columbus, OH, USA, 1999, pp. 323–329.

[5] M.W.A. Stewart, E.R. Vance, A. Jostsons, B.B. Ebbinghaus, J. Ceram. Soc. Aust. 39 (2003) 130–148.

[6] Y. Zhang, B.S. Thomas, G.R. Lumpkin, M. Blackford, Z. Zhang, M. Colella, Z. Aly, J. Nucl. Mater. 321 (2003) 1–7.

[7] Y. Zhang, K.P. Hart, W.L. Bourcier, R.A. Day, M. Colella, B. Thomas, Z. Aly, A. Jostsons, J. Nucl. Mater. 289 (2001) 254–262.

[8] Y. Zhang, K.P. Hart, M. Blackford, B. Thomas, Z. Aly, G.R. Lumpkin, M.W.A. Stewart, P. McGlinn, A. Brownscomb, in: K.P. Hart, G.R. Lumpkin (Eds.) Mater. Res. Soc. Symp. Proc. 663 (2001) 325–332.

[9] B.D. Begg, E.R. Vance, S.D. Conradson, J. Alloys Compd. 271–273 (1998) 221–226.

[10] B.D. Begg, E.R. Vance, B.A. Hunter, J.V. Hanna, J. Mater. Res. 13 (1997) 3181–3190.

[11] J.E. Patchett, E.W. Nuffield, Can. Mineral. 6 (1960) 483–490.

[12] K. Finnie, Z. Zhang, E.R. Vance, M.L. Carter, J. Nucl. Mater. 317 (2003) 46–53.

[13] M. Colella, G.R. Lumpkin, Z. Zhang, E.C. Buck, K.L. Smith, Phys. Chem. Miner. 32 (2005) 52–64.

[14] E.R. Vance, K.S. Finnie, Y. Zhang, B.D. Begg, in: J.M. Hanchar, S. Stroes-Gascoyne, L. Browning (Eds.) Mater. Res. Soc. Symp. Proc. 824 (2004) 249–254.

[15] W.T. Carnall, H.M. Crosswhite, Optical Spectra and Electronic Structure of Actinide Ions in Compounds and in Solution, ANL-84-90, Argonne National Laboratory, USA, 1985.

[16] J.C. Krupa, J. Alloys Compd. 225 (1995) 1–10.

[17] J. Blaise, M.S. Fred, W.T. Carnall, H.M. Crosswhite, H. Crosswhite, Plutonium Chemistry, in: W.T. Carnall, G.R. Choppin (Eds.), ACS Symposium Series 216, American Chemical Society, Washington, DC, 1983, pp. 173–198.

[18] J. Drozdzynski, K. Schwochau, H.J. Schenk, J. Inorg. Nucl. Chem. 43 (1981) 1845–1848.

[19] G.R. Lumpkin, K.L. Smith, M.G. Blackford, R. Giere, C.T. Williams, Micron 25 (6) (1994) 581–587.

[20] W.W. Wendlandt, H.G. Hecht, Reflectance Spectroscopy, Wiley Interscience, New York, 1966.

[21] J.H. Hadley Jr., F.H. Hsu, E.R. Vance, B.D. Begg, J. Am. Ceram. Soc. 88 (2005) 246–248.

[22] M.P. Lahalle, J.C. Krupa, R. Guillaumont, J. Less-Common Met. 122 (1986) 65–73.

[23] E.R. Vance, G.R. Lumpkin, M.L. Carter, D.J. Cassidy, C.J. Ball, R.A. Day, B.D. Begg, J. Am. Ceram. Soc. 85 (2002) 1853–1859.